VERTICAL MIXING OF MASS IN STABLY STRATIFIED CHANNEL FLOW WITH VERTICAL WALLS

Sutanu Sarkar
Department of Mechanical and Aerospace Engineering
Univ. of California San Diego
9500 Gilman Drive, La Jolla, CA 92093-0411, USA
sarkar@ucsd.edu

Vincenzo Armenio
Dipartimento di Ingegneria Civile
Universitá di Trieste
34127 Trieste, Italy
armenio@univ.trieste.it

ABSTRACT

Stably-stratified flow of water through a channel with infinite side walls is studied using large eddy simulation. Mean shear in the horizontal plane promotes turbulence while the orthogonal buoyancy force tends to inhibit vertical fluctuations. The variation of horizontal momentum transport and vertical mass transport as a function of the generalized Richardson number, a measure of stratification relative to shear, is obtained. It is found that turbulence remains three-dimensional allowing vertical transport. Although the vertical eddy diffusivity decreases with increasing value of the local gradient Richardson number, it is generally larger than that in the more typical situation of flow in a channel with vertical shear.

INTRODUCTION

It is well established that stable stratification inhibits vertical mixing of mass and momentum. In the case of a stratified medium undergoing vertical shear, a flow that has been thoroughly investigated in the past, it is known that the value $Ri_g \sim 0.25$ of the gradient Richardson number is key for demarcating zones characterized by sustained turbulence from other zones. However, in practice, there are several situations in environmental applications where stratification and shear are not aligned, in that there are significant horizontal gradients of mean velocity in a flow with a vertical density gradient. Although it is intuitively clear that horizontal transport in such a configuration could occur, it is unclear if a vertical fluctuations with associated buoyancy flux would survive in the presence of stable stratification. Fundamental studies of linear stability or of turbulence in such a configuration are lacking, perhaps due to the inherent three-dimensionality. Indeed, a two-dimensional analysis in the horizontal plane of shear would completely miss any vertical transport as well as any possible effect of vertical stratification on horizontal transport.

In vertical shear (VS) flow, the gradient Richardson number, $Ri_g = N^2/S^2$, is a fundamental local measure of the competing effects of stratification and shear on both linear instabilities and turbulence. In horizontal shear (HS) flow, although N is associated with vertical stratification while S is associated with horizontal shear orthogonal to the direction of stratification, introducing a quantity such as Ri_g makes sense if we interpret it as a squared ratio of two characteristic frequencies imposed on the unsteady motion, namely, the mean buoyancy, N, and the mean shear, S. Also, when the normalized equation for the turbulent kinetic energy is considered, Ri_g appears in both horizontal and vertical shear configurations. An effort to evaluate the effect of stable stratification in horizontal shear flow in the context of turbulence was made by Jacobitz and Sarkar (1999,2000) who performed DNS with *uniform* values for both mean shear and vertical stratification. It was found that, although turbulence was eventually suppressed in the case of uniform HS, the critical value of $Ri_g \simeq 2.0$ exceeds the value of $Ri_g \simeq 0.2$ corresponding to uniform VS. Also, the vertical mass diffusivity was generally larger in the HS configuration compared to the VS configuration.

Horizontal shear in applications often occurs near solid boundaries. However, the previous work of Jacobitz and Sarkar (1999,2000) considered uniform shear and stratification in an infinite domain without any boundaries. Instabilities and turbulence in wall-bounded flows, even without stratification, have qualitative differences with respect to those in uniform shear flow. The gradient Richardson number, Ri_g, is spatially constant in uniform shear flow and is identical to an overall Richardson number, Ri_b, based on velocity and density differences over a characteristic length scale. In contrast, wall-bounded flows have as a spatially-varying Ri_g which, by virtue of being small in the vicinity of walls, allows near-wall turbulence to persist even if $Ri_b = O(1)$. Based on these considerations, any direct extension of the previous studies by Jacobitz and Sarkar (1999,2000) to deduce the role of horizontal shear in wall-bounded stratified flows would be inappropriate. Therefore, we investigate here a different flow, a channel with vertical side walls. To the best of our knowledge, it is the first investigation to focus on mixing in a stratified medium by horizontal boundary shear.

PROBLEM DESCRIPTION

Flow of water through a channel with infinite vertical walls separated by a distance $2h$, and with a uniform vertical stratification is studied. From the schematic, Fig. 1, it is clear that the horizontal mean shear, $d < U > /dy$, is a function of the direction y, while the vertical stratification,

Case	Re_τ	Re_b	Ri_τ	Ri_b	$c_f \times 10^2$
$C0$	390	7320	0	0	0.60
$C1$	390	7350	7	0.021	0.59
$C2$	390	7500	15	0.044	0.57
$C3$	390	9025	100	0.20	0.39
$CV1$	390	8700	200	0.21	0.42
$CV2$	390	9380	400	0.36	0.36

Table 1: Parameters of the simulations and bulk quantities of the flow field. Cases C0-C3 correspond to horizontal shear channel flow while cases CV1 and CV2 correspond to vertical shear channel flow.

$d < \rho > /dz$, is imposed as a constant value. Consequently, all Reynolds-averaged turbulence statistics vary in *a single* direction of inhomogeneity, namely the y coordinate, and are obtained by averaging in the $x - z$ plane and in time. In particular, the buoyancy flux, $B =< \rho' w' >$ and the Reynolds shear stress, $< u'w' >$, vary only in the y direction and not in the z (vertical) direction. For future reference, we will use indicial notation ($i = 1, 2, 3$) instead of x, y, z when convenient. The friction Reynolds number, $Re_\tau = u_\tau h/\nu$ (based on the half width of the channel h and the friction velocity u_τ) is set to $Re_\tau = 390$ that, in the case of neutral flow, corresponds to a bulk Reynolds number (based on the bulk, area-averaged velocity of the flow, U_b) of $Re_b = U_b h/\nu \simeq 7300$. The Prandtl number, $Pr = 5$, corresponds to thermally-stratified water.

The governing equations are solved using the semi-implicit fractional step method of Zang *et al.* (1994). The spatial derivatives are discretized using second-order central differences, the time advancement is carried out using the Crank-Nicolson scheme for the diffusive term and the Adams-Bashforth technique for the convective terms. A multigrid technique is employed for the solution of the pressure equation. A nonuniform grid is used in the wall-normal y coordinate.

The SGS momentum flux is computed with a mixed model composed of a scale-similar part (Bardina *et al.* 1980) and an eddy viscosity one introduced by Smagorinsky (1963) using the dynamic procedure of Germano *et al.* (1992). The SGS buoyancy flux is modeled by means of a dynamic eddy-viscosity model as is performed for the evaluation of the constants. Unphysically large back-scattering is avoided by setting the coefficients to zero whenever they reach negative values. Details on the SGS models and the validation of the numerical algorithms in the stratified VS configuration are given by Armenio and Sarkar (2002). For the horizontal shear configuration, only the passive scalar case of Matsubara *et al.* (1998) at a Reynolds number, $Re_\tau = 150$, and Prandtl number, $Pr = 0.7$ is available. The first and second order statistics (not reported here) obtained by LES compare well with the reference DNS data of Matsubara *et al.* (1998).

The domain is chosen to be $2\pi h$ in the streamwise direction, πh in the vertical direction and $2h$ in the wall-normal direction. The grid used has $64 \times 96 \times 64$ cells in the streamwise, wall-normal and vertical directions, respectively. Four cases are simulated: a passive scalar case (C0) in which the velocity field is not affected by the evolution of the density field and three cases (C1,C2,C3) with progressively increasing values of N. The cases investigated are reported in Table 1.

In order to place the results of HS channel flow in context of the more typical case of vertical shear, we have also performed two additional computations of VS channel flow at the same values of Reynolds number, $Re_\tau = 390$, and Prandtl number, $Pr = 5$. In both VS and HS cases, the mean flow is sustained by a mean, driving, pressure gradient. The stable stratification is maintained in the VS configuration by setting the upper wall at a density lower than that of the lower wall so that, unlike the HS case, the mean density gradient and associated Brunt-Vaisala frequency N evolve with the flow and are *not* held constant. The VS simulations have been carried out using 64×64 grid points in the streamwise and spanwise directions, respectively, while the vertical direction has 128 points. In the case of vertical shear, the bulk Richardson number is defined as $Ri_b = g\Delta\rho h/2\rho_0 u_b^2$, where $\Delta\rho$ denotes the density difference that is imposed between the upper and lower walls, and similarly, the friction Richardson number is defined by $Ri_\tau = g\Delta\rho h/\rho_0 u_\tau^2$.

As discussed in the introduction, the gradient Richardson number, $Ri_g = N^2/S^2$, is a fundamental local measure of the competing effects of mean shear that promotes turbulence and mean stratification that tends to suppress turbulence. Fig. 2 shows the variation of Ri_g as a function of wall-normal distance, y/h in the case of HS channel flow and z/h in the case of VS channel flow. There is an important qualitative difference between VS and HS cases: for the same overall stratification (Ri_τ or Ri_b), the gradient Richardson number, Ri_g, is generally larger in the HS case at a given distance from the wall. Even HS case C1 with the smallest value of $Ri_b = 0.021$ has $Ri_g(z)$ that is generally larger than VS case CV2 with the largest value of $Ri_b = 0.36$. This is a consequence of the fact that, in the HS configuration, N is held constant while, in the VS configuration, turbulence near the wall is able to mix up the density field in the mean reducing the local value of N and therefore $Ri_g = N^2/S^2$.

VELOCITY STATISTICS

Figure 3 shows the mean velocity profile as a function of the distance from the wall, for several cases of stratification. The driving mean pressure gradient is not changed between the cases and therefore, as shown by Fig. 3, the wall shear stress, equivalently, the slope of the mean velocity profile at the wall is also unchanged. Figure 3 also shows that the velocity field is very weakly affected by stratification in cases C1 and C2, whereas a stronger change of the velocity profile is observed in case C3. Thus, when stratification acts in a direction normal to the plane of flow, it can alter the mean velocity field only if it is rather large.

The turbulent intensities are reported in Fig. 4. It is clear that there is a noticeable reduction of the level of fluctuations as the stratification increases with the suppression of the vertical as well as the wall-normal fluctuations being more intense than that of the streamwise fluctuation, that is almost unaffected by stratification. This can be explained looking at the transport equation for the Reynolds stress tensor. Among the three velocity components, stratification directly affects *only* the vertical Reynolds stress $< w''^2 >$, through the destruction supplied by the buoyancy term $B = Ri < \rho'' w'' >$. Therefore, the vertical fluctuating field is somewhat suppressed by stratification, (Fig. 4c), whereas the streamwise Reynolds stress is very weakly influenced by stratification (Fig. 4a) since the production term $P_{u^2} = - < u''v'' > d < u > /dy$ is nearly unchanged.

Thus, it appears that, for the stratified cases considered here, the vertical turbulence level remains substantial and stratification is not able to two-dimensionalize the fluctuating motion. Horizontal fluctuating vorticity (not shown

here) remains substantial and so does the pressure-strain (not shown here) component in the transport equation for the vertical fluctuation.

COMPARISON OF HS AND VS CASES

In the previous uniform-shear simulations, the value of Ri_g was constant in any given case because so were N and S making it easy to compare HS and VS cases. Here, the Ri_g profiles are qualitatively different as indicated by Fig. 2 and the accompanying discussion and, therefore, direct comparison between HS and VS configurations is not possible. As an alternative, we discuss profiles of key quantities as a function of Ri_g so as to, first, identify key differences between HS and VS cases and, second, to explore the role of Ri_g in identifying stratification effects on turbulent transport.

The vertical eddy diffusivity, k_T, of mass is compared between HS and VS configurations in Fig. 5. Normalization is with respect to the molecular viscosity which is identical between all cases. In the stratified region, $Ri_g > 0.1$, the values of k_T are generally much larger in the HS configuration relative to the VS configuration. Apparently, the fluctuating vertical shears associated with mean horizontal shear are more effective in overcoming the stabilizing influence of stratification than those associated with mean vertical shear. In the vicinity of the wall, again the HS configuration is more effective in mediating vertical transport. The reason is now different; the vertical velocity in the HS configuration is spanwise while it is wall-normal in the VS configuration and, going away from the wall, the spanwise component (linear variation) increases faster from zero than the wall-normal component (quadratic variation).

Finally, we show two relevant quantities, namely the correlation coefficient of the vertical buoyancy flux

$$C_{\rho w} = \frac{< \rho' w' >}{\rho_{rms} w_{rms}}$$

and the correlation coefficient of the wall-normal momentum flux

$$C_{uv_n} = \frac{< u' v_n' >}{u_{rms} v_{n,rms}},$$

with v_n denoting the wall-normal component of the velocity field. Figure 6 shows $C_{\rho w}$ plotted against the local parameter Ri_g for the VS case and the HS case. The behavior is qualitatively similar in all cases. In particular, it is relatively constant in the region of small values of Ri_g, it decays when Ri_g reaches a critical value and, beyond that, $C_{\rho w}$ rapidly goes to 0. In spite of this qualitative similarity, important differences occur between HS and VS configurations; the most important is that the value of Ri_g required for the correlation coefficient to decay is one order of magnitude smaller in the VS cases compared to the HS cases. Indeed, in the VS configuration, the correlation coefficient sharply decays to zero in the vicinity of $Ri_g \simeq 0.2$, similar to the behavior observed by Armenio and Sarkar (2002) even though the Peclet number $Pe_\tau = Re_\tau Pr$ in that study was smaller than that of the present investigation by a factor of 10. In the horizontal-shear case, we do not observe a sharp reduction of the correlation coefficient at $Ri_g \simeq 0.2$; rather, there is a gradual decrease of the correlation coefficient and it approaches zero at values of $Ri_g \simeq 2$, an order of magnitude larger than VS channel flow. Furthermore, in the VS configuration, the coefficient gets negative in the range of large values of Ri_g, due to the observed counter-gradient fluxes. On the other hand, in the HS configuration, positive values of $C_{\rho w}$ are obtained in all the cases simulated.

The behavior of the correlation coefficient of momentum flux is completely different in the HS case compared to the VS case. Figure 7(a) shows the coefficient C_{uv_n} as a function of the gradient Richardson number. In the VS configuration, this coefficient is qualitatively similar to that of the buoyancy flux, in that it is nearly constant for small values of Ri_g, it dramatically decreases near $Ri_g \sim 0.2$ and tends to 0 as the gradient Richardson number further increases. Thus, it exhibits a universal behavior, when plotted against Ri_g, for example, compare curves $C1V$ and $C2V$ of Fig. 7(a) of the present work, Fig. 20 of Armenio and Sarkar (2002) and Fig. 7 of Komori *et al.* (1983) obtained for different values of the Peclet number. Furthermore, in the VS configuration, the coefficient exhibits a weak dependence on the overall stratification, quantified for example by Ri_τ or Ri_b, in that, at a given value of the local parameter Ri_g, the coefficient slightly decreases with increasing stratification.

In the HS cases, the correlation coefficient of the momentum flux, C_{uv_n}, behaves very differently; in particular, when it is plotted against the gradient Richardson number (Fig. 7a) we do not observe any collapse between cases, rather, we note that the value of Ri_g at which the coefficient starts to decrease, increases with stratification. It is clear that the local parameter Ri_g is not the proper one for the characterization of C_{uv_n}. In contrast, when the coefficient is plotted against $y^+ = yu_\tau/\nu$ (Fig. 7b), we observe that the coefficient collapses over a very narrow range of values in all three cases examined. In particular, independent of the level of stratification, the coefficient rapidly increases in the near wall layer (up to $y^+ = 10$), it has a saddle-like behavior in the buffer layer ($10 < y^+ < 50$), it is nearly constant in the *log*-layer and then decreases to 0 in the core region of the boundary layer. The final decrease to zero in the core region is simply because the mean shear relaxes to zero at the centerline. Thus, insofar as horizontal momentum transport is concerned, stable stratification in the range studied here has little effect on the relevant correlation coefficient.

PARAMETERIZATION OF VERTICAL TRANSPORT

The objective here is to derive a simple *algebraic* relationship for the vertical eddy diffusivity of mass, k_T, that can be used to estimate the vertical mixing from measurements of the mean velocity and density in the HS configuration.

The starting point of the present parameterization is that the vertical eddy diffusivity can be written, *without* any approximation, as:

$$k_T = -\frac{< \rho' w' >}{d < \rho > /dz} = C_{\rho w} L_E w_{rms} = \frac{C_{\rho w} w_{rms}^2}{N Fr_w} \qquad (1)$$

where, as defined previously, $C_{\rho w}$ denotes the correlation coefficient of the buoyancy flux, $L_E = \rho_{rms}/(d < \rho > /dz)$ is the Ellison length scale, and $Fr_w = w_{rms}/NL_E$ is the vertical turbulent Froude number. In our LES, we observe the presence of two separate regions away from the viscous wall region, namely an inner, buoyancy influenced (BI) region with small values of Ri_g and an outer, buoyancy dominated (BD) zone with large values of Ri_g. The BI zone, with generally larger k_T relative to the BD region, has the peak value of k_T. The extent of these two zones depends on the overall level of stratification and they merge with each other in a zone where the gradient Richardson number $Ri_g = O(1)$.

First, consider the *buoyancy-dominated* outer region, $Ri_g > 0.5$. Here, the vertical Froude number does not depend on the overall level of stratification (Ri_b or Ri_τ) and the asymptotic value is $Fr_w = 0.8$ for all cases investigated.

Also, Fig. 4(c) suggests that the vertical turbulent intensity in the outer layer can be approximated by $w_{rms}/u_\tau \simeq 0.5$, in cases C1 to C3. With these values in Eq. (1), the value of the eddy diffusivity in the BD region reads as:

$$k_{T,BD} = 1.25 C_{\rho w} \frac{w_{rms}^2}{N} \simeq 0.31 C_{\rho w} \frac{u_\tau^2}{N} . \qquad (2)$$

We emphasize that $C_{\rho w}$ is not constant, see Fig. 6, and it decreases with increasing Ri_g in the outer layer so that k_T decreases faster than $1/N$ in the BD region. Eq. (2) belongs to the following family of models suggested by simple dimensional analysis:

$$k_T = c_N \frac{w_{rms}^2}{N} , \qquad (3)$$

where the proportionality coefficient was originally taken to be approximately constant, $c_N \simeq 0.16$, by Hunt *et al.* (1995), but later recognized to be a function of Ri_g, for example, by Schumann and Gerz (1995) based on VS data in the atmospheric boundary layer data and uniform shear flow. The present LES data support Eq. (3) in the BD region with c_N a decreasing function of Ri_g and a maximum value of $c_N \simeq 0.3$.

Now, consider the *buoyancy-influenced* region. In the buoyancy-influenced (BI) zone, Eq. (2) predicts smaller values of k_T relative to the LES data and requires modification. We find that the peak diffusivity varies as

$$k_{T,peak} = 0.4 Ri_\tau^{0.25} C_{\rho w} \frac{u_\tau^2}{N} , \qquad (4)$$

where w_{rms} has taken to be proportional to u_τ. The eddy diffusivity model in the BI region must match that in the BD region and, therefore, the parameterization becomes:

$$k_T = f_w \left[(k_{T,peak} - k_{T,BD}) f(Ri_g) + k_{t,BD} \right] \qquad (5)$$

where $f(Ri_g) = 1$ as $Ri_g \to 0$ to match the peak value of the BI layer, and $f(Ri_g) \to 0$ as $Ri_g \to \infty$ to match the BD layer. The following function,

$$f(Ri_g) = \frac{1}{1 + 50 Ri_g^4} , \qquad (6)$$

fitted over the present LES data, has been found to work satisfactorily.

In order to go further with the parameterization, we need an analytical expression for the correlation coefficient, $C_{\rho w}$. An analytical expression that fits well the curves of Fig. 6 for cases C1 to C3 is:

$$C_{\rho w} = \frac{C_{\rho w,peak}}{1 + Ri_g} = \frac{0.2 + 0.1 exp(-0.1 Ri_\tau)}{1 + Ri_g} . \qquad (7)$$

The term in the numerator represents the observed fact that the peak value of the correlation coefficient decreases somewhat from case C0 to C3 at a constant value of Ri_g.

Finally, we consider the *viscous layer* adjacent to the wall where molecular effects are directly important. Since the buoyancy flux $B = 0$ at the wall, such is the eddy diffusivity. Therefore, the parameterized k_T needs to multiplied by a damping function in the viscous region of the boundary layer similar to the van Driest damping function that is widely used in wall-turbulence modeling. A damping function that fits the present LES data is:

$$f_w = 1 - exp(-0.09 y^+) . \qquad (8)$$

Eq. (8) ensures that $f_w = 0$ at the wall and goes to unity at the edge of the viscous near-wall region, $y^+ \simeq 30$.

Thus, the complete parameterization is:

$$k_T = C_{\rho w} \frac{u_\tau^2}{N} [0.31 - 0.4 Ri_\tau^{0.25} f(Ri_g)] f_w \qquad (9)$$

with $C_{\rho w}(Ri_g, Ri_\tau)$, $f_w(y^+)$ and $f(Ri_g)$ defined by Eq. (7), (8) and (6), respectively.

Fig. 8 shows wall-normal profiles of the eddy diffusivity, k_T. The BD model, Eq. (2), valid for $Ri_g > 0.5$, is a good representation of the outer layer which ranges from a small physical extent, $y/h > 0.75$, in case C1 to a larger region, $y/h > 0.4$, in case C3 with stronger stratification. Fig. 8(b) shows the performance of the composite parameterization, Eq. (9), over the channel half width. Given the large variation of Ri_g in any given case and the large change in N^2 by an order of magnitude between cases, the agreement between the parameterization and the LES data is good.

CONCLUSIONS

The primary question is whether the horizontal mean shear associated with the vertical side walls can mediate vertical mass transport against stable stratification. It is found that the fluctuating motion remains three-dimensional and the vertical component has an associated buoyancy flux. Although, the mean vorticity is vertical, there are regions of strong horizontal fluctuating vorticity which can induce rotational motion in the vertical plane and thereby mixing of the density field. There are many indicators that mean horizontal shear (HS) is more effective in promoting vertical buoyancy fluxes than mean vertical shear (VS) in stably-stratified regions of the flow. The increased eddy diffusivity and the increased range of Ri_g over which the density-velocity correlation coefficient is greater than zero are two such indicators. Profiles of the Ellison length scale and the mixing efficiency, B/ϵ, not shown here, are also indicative of increased vertical transport associated with HS.

To interpret field or laboratory data, it is useful to relate the eddy diffusivity to observable mean data. To that end, a simple parameterization, based on the LES data and guiding physical principles, is proposed.

REFERENCES

Armenio V. & Sarkar S., 2002, " An investigation of stably-stratified turbulent channel flow using large eddy simulation," *J. Fluid Mech.* **459**, 1.

Bardina, J., Ferziger, J. H., & Reynolds, W. C., 1980, "Improved subgrid scale models for large eddy simulation," *AIAA paper No. 80-1357.*

Hunt, J. C. R., Kaimal, J. C. & Gaynor, J. E., 1985, "Some observations of turbulence structure in stable layers," *Quart. J. Royal Meteor. Soc.* **111**, 793-815.

Jacobitz F. G. & Sarkar, S., 1999, "The effect of nonvertical shear on turbulence in a stably stratified medium," *Phys. Fluids*, **10**, 1158.

Jacobitz F. G. & Sarkar, S., 2000, "Turbulent Mixing in a Vertically Stably Stratified Fluid with Uniform Horizontal Shear," *Flow, Turbulence and Combustion*," **63**, 343-360.

Komori S., Ueda H., Ogino F. & Mizushina T., 1983, "Turbulent structure in stably stratified open-channel flow," *J. Fluid Mech.* **130**, 13.

Matsubara K., Kobayashi, M. & Maekawa, H., 1998, "Direct numerical simulation of a turbulent channel flow

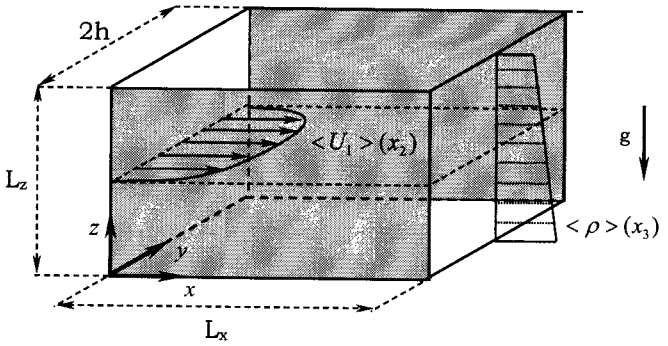

Figure 1: Problem schematic of channel flow with horizontal shear. Water flows through a channel between parallel vertical walls separated by a distance $2h$. The medium is stably stratified with a constant mean density gradient. The mean shear and mean density gradient are orthogonal in this problem.

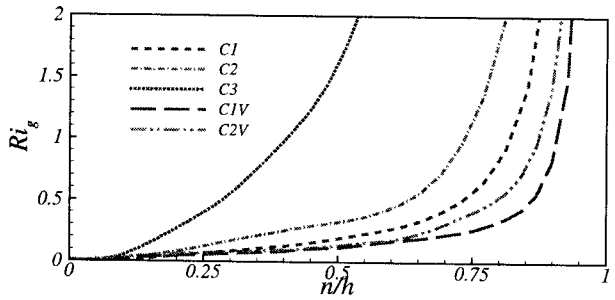

Figure 2: Wall-normal distribution of the gradient Richardson number for several levels of stratification in the horizontal shear case and in the vertical shear case (n denotes the wall-normal direction).

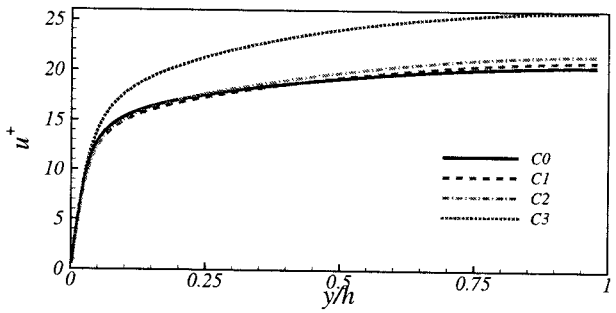

Figure 3: Mean velocity profiles for several levels of stratification.

with a linear spanwise mean temperature gradient," *Int. J. Heat Transfer*, **41**, 3627.

Schumann, U. and Gerz, T., 1995, "Turbulent mixing in stably stratified shear flows," *J. Appl. Meteor.*, **34**, 33.

Smagorinsky, J., 1963, "General circulation experiments with the primitive equations. I The basic experiment," *Monthly Weather Review*, **91**, 99.

Zang, Y., Street, R. L. & Koseff, J., 1994, "A non-staggered grid, fractional step method for the time-dependent incompressible Navier-Stokes equation in curvilinear coordinates," *J. Comput. Phys.* **114**, 18.

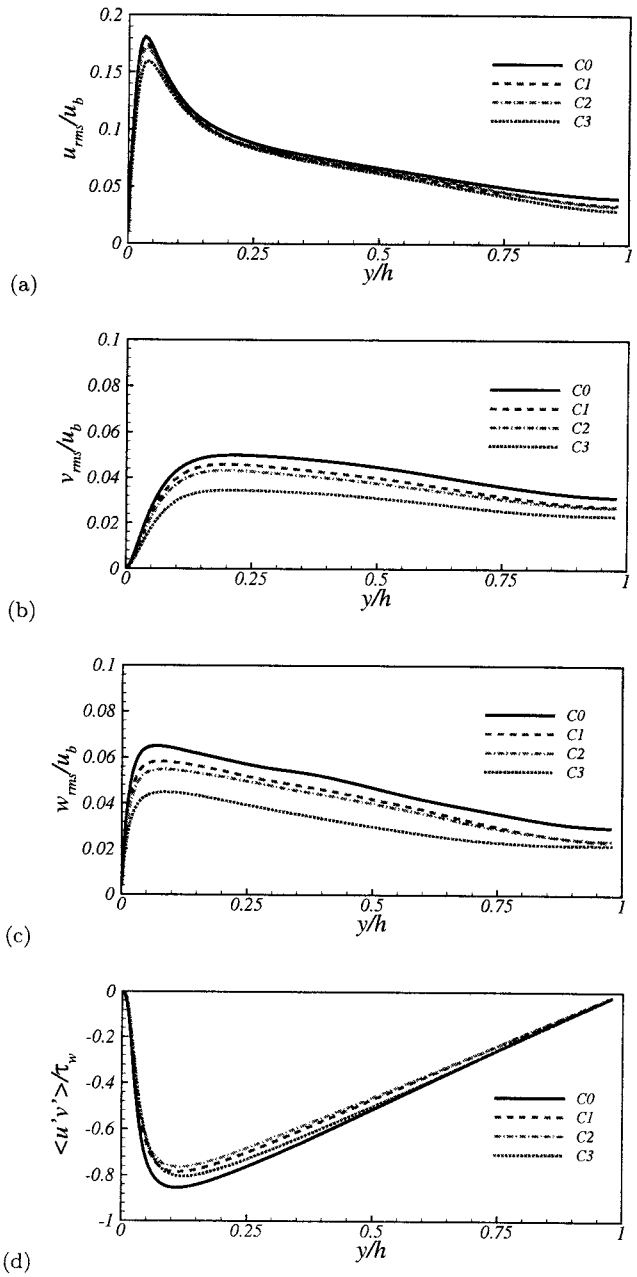

Figure 4: Turbulent levels for several levels of stratification: a)streamwise, b)wall-normal, c)vertical, and d) shear stress.

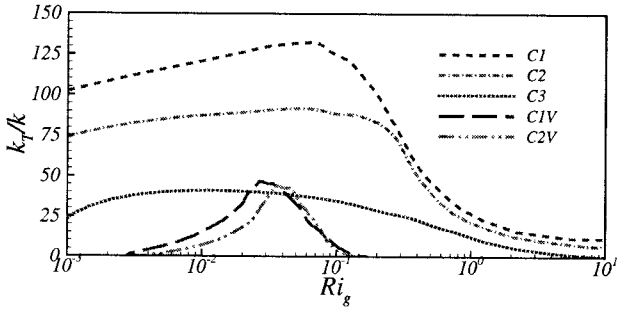

Figure 5: Vertical eddy diffusivity of mass for several levels of stratification in the horizontal shear case and in the vertical shear case.

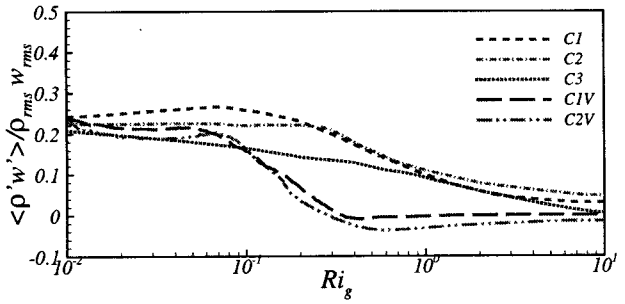

Figure 6: Correlation coefficient of the buoyancy flux versus the gradient Richardson number for several levels of stratification in the HS case and in the VS case

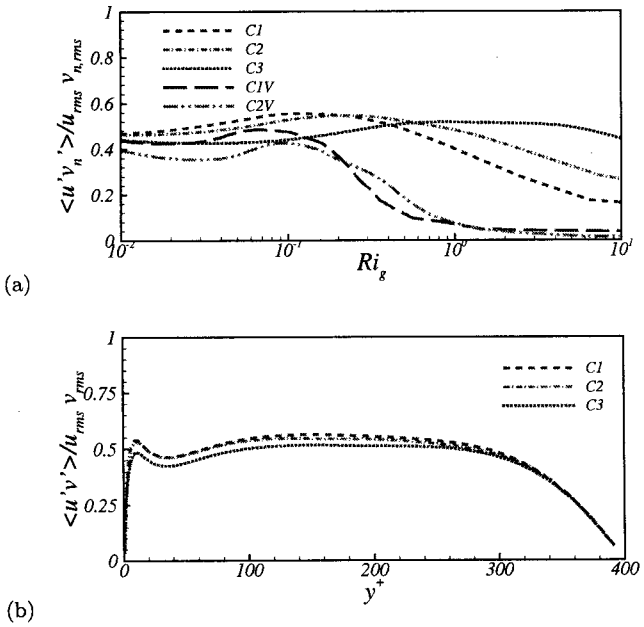

Figure 7: Correlation coefficient of wall-normal momentum flux, plotted against: a) gradient Richardson number, b) nondimensional distance from the wall.

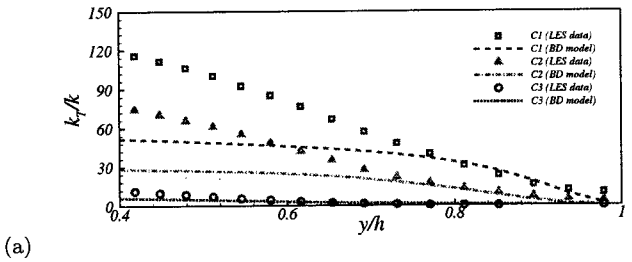

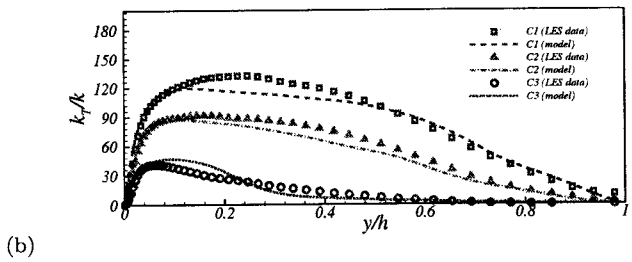

Figure 8: Wall-normal profile of eddy diffusivity obtained with the proposed parameterization along with LES data of HS channel flow. (a) The BD component, Eq. (2), in the outer region, (b) The composite parameterization, Eq. (9), over channel half-width.